Inverse Problems

PAPER

Lipschitz stability for an inverse source scattering problem at a fixed frequency*

To cite this article: Peijun Li *et al* 2021 *Inverse Problems* **37** 025003

IOP Publishing Inverse Problems

Inverse Problems 37 (2021) 025003 (17pp) https://doi.org/10.1088/1361-6420/abd3b4

Lipschitz stability for an inverse source scattering problem at a fixed frequency*

Peijun Li[1], **Jian Zhai**[2,**] and **Yue Zhao**[3]

[1] Department of Mathematics, Purdue University, West Lafayette, Indiana 47907, United States of America
[2] Institute for Advanced Study, The Hong Kong University of Science and Technology, Kowloon, Hong Kong, People's Republic of China
[3] School of Mathematics and Statistics, Central China Normal University, Wuhan 430079, People's Republic of China

E-mail: lipeijun@math.purdue.edu, iasjzhai@ust.hk and zhaoyueccnu@163.com

Received 20 July 2020, revised 14 December 2020
Accepted for publication 15 December 2020
Published 5 January 2021

Abstract
This paper is concerned with an inverse source problem for the three-dimensional Helmholtz equation by a single boundary measurement at a fixed frequency. We show the uniqueness and a Lipschitz-type stability estimate under the assumption that the source function is piecewise constant on a domain which is made of a union of disjoint convex polyhedral subdomains.

Keywords: inverse source problem, the Helmholtz equation, stability

(Some figures may appear in colour only in the online journal)

1. Introduction

The inverse source scattering problems arise in diverse scientific and industrial areas such as antenna design and synthesis, medical imaging [28]. In general there is no uniqueness for the inverse source scattering problems with the boundary data at a fixed frequency [20]. This is clear since a single near-field or far-field measurement gives a function of $n-1$ independent variables in an n-dimensional space, while the source function has n independent variables. An effective approach to overcome the non-uniqueness issue is the use of multi-frequency data.

*The research of PL is supported in part by the NSF Grant DMS-1912704.

**Author to whom any correspondence should be addressed.

More interestingly, the use of multi-frequency data may enhance the stability of the problems [1, 7–10, 24, 33, 34].

Nevertheless, with single-frequency data, it is proved in [32, 39] that the support of the source can still be determined in certain cases. In [31], it was shown that the convex hull of a polygonal source can be determined from a single measurement. For sources with a convex polygonal support, it has been proved that the support and the values of the source function at corner points can be uniquely determined by a single measurement in homogeneous [17] and inhomogeneous media [30]. In [19], the authors addressed the absence of real non-scattering energies by examining the phenomenon that corners always scatter. Related studies can be found in [26, 27] on the uniqueness of the shape identification by using a single measurement in the inverse conductivity and medium scattering problems, respectively. We refer to [5, 6] for the uniqueness and numerical results for recovering point and dipole sources.

Consider the three-dimensional Helmholtz equation

$$\Delta u(x) + \kappa^2 u(x) = f(x), \quad x \in \mathbb{R}^3, \tag{1}$$

where $\kappa > 0$ is the wavenumber, u denotes the wave field, and the source function $f \in L^\infty(\mathbb{R}^3)$ represents the electric current density and is assumed to have a compact support contained in a bounded domain $\Omega \subset \mathbb{R}^3$ with a connected complement $\mathbb{R}^3 \setminus \overline{\Omega}$. Furthermore, we assume that $\overline{\Omega} \subset B_R := \{x \in \mathbb{R}^3 : |x| < R\}$, where $R > 0$ is a constant. The wave field u is required to satisfy the Sommerfeld radiation condition

$$\lim_{r\to\infty} r(\partial_r u - \mathrm{i}\kappa u) = 0, \quad r = |x| \tag{2}$$

uniformly in all directions $\hat{x} = x/|x|$.

Given the source f, the direct scattering problem is to determine the wave field u which satisfies (1) and (2). It is known that the direct scattering problem has a unique solution $u \in H^2(B_R)$ for an arbitrary wavenumber $\kappa > 0$ and the solution u satisfies the following estimate (cf [25]):

$$\|u\|_{H^2(B_R)} \leqslant C\|f\|_{L^\infty(\Omega)}, \tag{3}$$

where C is a positive constant. This paper is concerned with the inverse source scattering problem, which is to determine f from the boundary measurement of u on $\partial B_R = \{x \in \mathbb{R}^3 : |x| = R\}$ at a fixed wavenumber κ.

In this work, we consider the case where the source f is a piecewise constant function. More precisely, we assume

$$f(x) = \sum_{j=1}^{N} c_j \chi_{D_j}(x), \tag{4}$$

where D_j, $j = 1, \ldots, N$ are known disjoint convex polyhedral domains and c_j, $j = 1, \ldots, N$ are unknown constants. The goal is to establish the Lipschitz stability of determining the constants c_j, $j = 1, \ldots, N$ from the measurement of u on ∂B_R at a fixed wavenumber κ. It is known that there exist certain sources that produce no measurable signals, and those sources are called non-radiating sources [20]. However, since the support of the source function (4) has corners, it is a radiating source (cf [17]). This makes the recovery of f possible. We refer to [1, 2] for the characterization of radiating and non-radiating sources for the Helmholtz equation and Maxwell equations.

Our study is motivated by the idea introduced by Alessandrini and Vessella in [4], where the electrical impedance tomography problem was studied. This approach was further developed to study various inverse coefficient problems (cf, [3, 12–16]). In this paper, we use similar ideas to solve our inverse source problem. In [17, 31], the inverse source problems are studied by using complex geometric optics solutions, which are also typical mathematical tools for the inverse coefficient problems [22, 40].

We construct singular solutions and utilize their 'blow-up' behaviors near the corners of subdomains D_j, $j = 1, 2, \ldots, N$. The quantitative estimate of unique continuation of the solution for the Helmholtz equation, which is derived from a three spheres inequality, plays an essential role in the procedure. We derive a logarithmic-type stability for recovering $c_1, c_2, \ldots, c_N$, and then uniqueness follows immediately. Since we are recovering a finite number of unknowns, the Lipschitz-type stability estimate is obtained. Comparing with the uniqueness results in [17, 30], we provide the uniqueness for a different class of source functions and achieve the optimal stability estimate. We also want to point out that recently there are numerous results of establishing Lipschitz stability for some inverse problems using finite measurements (cf [2, 29, 35, 38] for the Calderón problem and [18] for inverse scattering problems).

The paper is organized as follows. In section 2, we summarize the main results. Section 3 is devoted to the proof of the main result. The paper is concluded with some general remarks and directions for future work in section 4.

2. Main result

In this section, we make some extra assumptions on the source function and state the main result of this work.

2.1. Geometry setup

Let the piecewise constant source function be given as

$$f(x) = \sum_{j=1}^{N} c_j \chi_{D_j}(x), \qquad \overline{\Omega} = \cup_{j=1}^{N} \overline{D}_j,$$

where $c_j \in \mathbb{C}$ are constants, and D_j are mutually disjoint bounded open subsets in $\mathbb{R}^3$. Assume that $\mathrm{dist}(\Omega, \mathbb{R}^3 \setminus B_R) \geqslant r_0$ for some constant $r_0 > 0$. Moreover, we consider the geometric setup of the domains D_j that can be described as the polyhedral cell geometry as follows (cf [18]).

Assumption 1. We assume that

(a) the subdomains $D_j \subset \mathbb{R}^3$, $1 \leqslant j \leqslant N$ are convex polyhedrons;
(b) for each $k = 0, \ldots, N-1$, $\cup_{j=k+1}^{N} \overline{D_j}$ is simply connected, and there exists a constant r_0 such that $\{x \in \mathbb{R}^3 | \mathrm{dist}(x, \cup_{j=k+1}^{N} \overline{D_j}) > 2r_0\}$ is connected;
(c) each D_j has a vertex, denoted by $P^{(j)}$, such that $B_{3r_0}(P^{(j)}) \cap D_k = \emptyset$ for any $k > j$.

An example domain in $\mathbb{R}^2$ satisfying the above assumptions is illustrated in figure 1.

Let (x_1, x_2, x_3) be the Cartesian coordinate in $\mathbb{R}^3$, and introduce the spherical coordinates

$$x_1 = \rho \sin\theta \cos\varphi, \qquad x_2 = \rho \sin\theta \sin\varphi, \qquad x_3 = \rho \cos\theta.$$

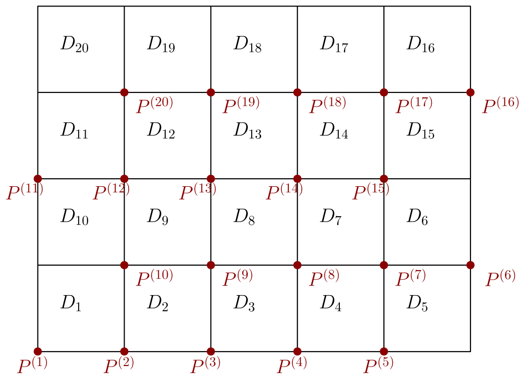

Figure 1. An example of the domain.

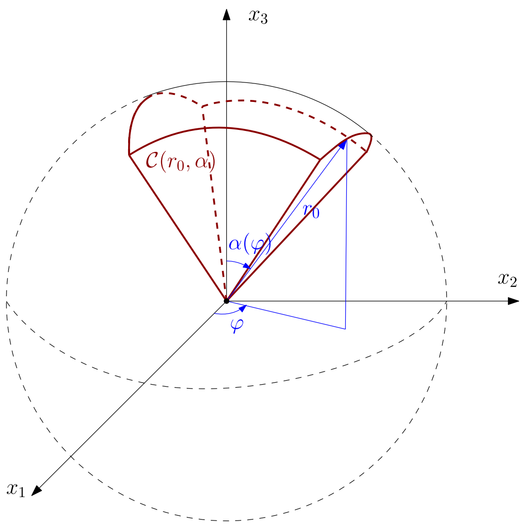

Figure 2. Illustration of $\mathcal{C}(r_0, \alpha)$.

Assume $\alpha = \alpha(\varphi)$ is a continuous function on $[0, 2\pi]$, such that $\alpha(\varphi) \in (0, \frac{\pi}{2})$ for any $\varphi \in [0, 2\pi]$. We let

$$\mathcal{C}(r_0, \alpha) := \{(\rho, \theta, \varphi) : 0 \leqslant \rho \leqslant r_0,\ 0 \leqslant \theta \leqslant \alpha(\varphi), 0 \leqslant \varphi \leqslant 2\pi\}$$

denote the cone with radius r_0 and vertical angle α. The vertex of the cone is the origin and the axis is the x_3-axis. The cone $\mathcal{C}(r_0, \alpha)$ is depicted in figure 2.

Assumption 2. Let α_1, α_2 be two constants satisfying $0 < \alpha_1 < \alpha_2 < \frac{\pi}{2}$. For each D_j, $j = 1, 2 \ldots, N$, let $P_\ell^{(j)}$ be a vertex. Assume that, after a rigid transform, $P_\ell^{(j)} = (0, 0, 0)$, and $B_{r_0} \cap D_j = \mathcal{C}(r_0, \alpha_\ell^{(j)})$ with $\alpha_1 < \alpha_\ell^{(j)}(\varphi) < \alpha_2$ for any $\varphi \in [0, 2\pi]$.

In addition, we also make the following assumption on the source function.

Assumption 3. The source function f has the compact support $\overline{\Omega}$ with $|\Omega| \leqslant A$ and satisfies $\|f\|_{L^\infty(\Omega)} \leqslant E$, where A and E are positive constants.

2.2. Statement of the main result

Denote

$$\epsilon := \|u\|_{H^1(\partial B_R)}.$$

The following theorem is the main result of this paper.

Theorem 1. *Let f satisfy assumptions 1–3 and the subdomains $D_j, j = 1, \ldots, N$ are given. If $\epsilon = 0$ then $f = 0$. Moreover, the following estimate holds:*

$$\|f\|_{L^\infty(\Omega)} \lesssim \epsilon. \tag{5}$$

Hereafter, the notation $a \lesssim b$ stands for $a \leqslant Cb$, where $C > 0$ is a positive constant which depends on the following parameters: $\kappa, A, E, N, r_0, R, \alpha_1, \alpha_2$.

Remark 1. We mention that the Lipschitz constant in the estimate (5) grows exponentially with respect to the number of subdomains N, which means that the stability estimate deteriorates dramatically as N grows. We refer to [13, 37] for related studies of this behavior. The Lipschitz constant also deteriorates when the number r_0 decreases due to the instability of the unique continuation principle and the use of increased number of three spheres inequalities.

2.3. Construction of singular solutions

To prove the theorem, we need to construct singular solutions to the Helmholtz equation and use their asymptotic behaviors near the singularities. For the inverse coefficient problems considered in [3, 4, 12–16], typically one may deal with a product of two singular solutions, whose positivity can be guaranteed. For our inverse source problem, we deal with only one singular solution, and therefore more sophisticated analysis is needed. In particular, we need to derive a lower bound on the integral of the singular solution over a cone, when the singular point is outside the cone and close to the vertex. One will see that the cone has to be strictly convex at the vertex in order to have such a bound. Since this is the key difference from previous work on the inverse coefficient problems, we provide more details in this section.

Denote by $G(x) = \frac{\mathrm{e}^{\mathrm{i}\kappa|x|}}{|x|}$ the fundamental solution to the three-dimensional Helmholtz equation in a homogeneous medium. By simple calculations, we obtain for sufficiently small $|x|$ that

$$\begin{aligned}\partial_{x_3}^3 \frac{\mathrm{e}^{\mathrm{i}\kappa|x|}}{|x|} &\sim \left(\frac{3x_3}{|x|^5} + \frac{6x_3}{|x|^5} - \frac{15x_3^3}{|x|^7}\right)\mathrm{e}^{\mathrm{i}\kappa|x|} + \mathcal{O}(|x|^{-3}) \\ &= \frac{x_3(9x_1^2 + 9x_2^2 - 6x_3^2)}{|x|^7}\mathrm{e}^{\mathrm{i}\kappa|x|} + \mathcal{O}(|x|^{-3}).\end{aligned}$$

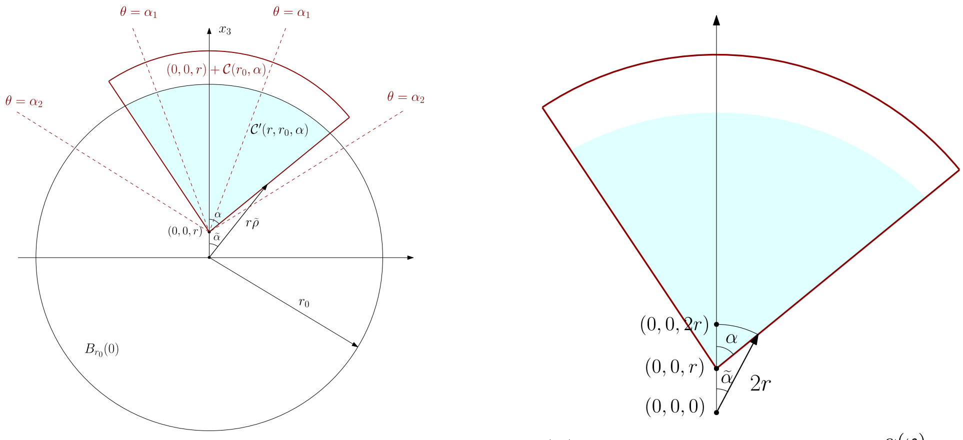

(A) Illustration of $\mathcal{C}(r_0, \alpha)$ and $\mathcal{C}'(r, r_0, \alpha)$.

(B) One can see clearly that $\frac{\alpha(\varphi)}{2} < \widetilde{\alpha}(\varphi, \widetilde{\rho}) < \alpha(\varphi)$ for $\widetilde{\rho} > 2$.

Figure 3. Illustrations of the domains defined.

We will use the following singular solution

$$\begin{aligned}\Phi(x) &= -\operatorname{Im}\left(\partial_{x_3}^3 \frac{\mathrm{e}^{\mathrm{i}\kappa|x|}}{|x|}\right)\\ &= \frac{x_3(-9x_1^2 - 9x_2^2 + 6x_3^2)}{|x|^7}\cos(\kappa|x|) + \mathcal{O}(|x|^{-3})\\ &= \frac{x_3(-9x_1^2 - 9x_2^2 + 6x_3^2)}{|x|^7} + \mathcal{O}(|x|^{-3}),\end{aligned} \tag{6}$$

which has a singularity at $x = 0$.

Consider a cone $\mathcal{C}(r_0, \alpha) = \{(\rho, \theta, \varphi) : 0 \leqslant \rho \leqslant r_0, 0 \leqslant \theta \leqslant \alpha(\varphi), 0 \leqslant \varphi \leqslant 2\pi\}$, with $\alpha_1 < \alpha(\varphi) < \alpha_2$ for any $\varphi \in [0, 2\pi]$. We assume that $0 < \alpha_1 < \alpha_2 < \frac{\pi}{2}$, and then the cone $\mathcal{C}(r_0, \alpha)$ is convex near the vertex. For our purpose, one can think this vertex as a corner of some D_j. Denote

$$\mathcal{C}'(r, r_0, \alpha) := B_{r_0}(0) \cap \{(0, 0, r) + \mathcal{C}(r_0, \alpha)\}.$$

See figure 3(A) for an illustration. Substitute

$$x_1 = r\widetilde{\rho}\,\sin\widetilde{\theta}\,\cos\varphi, \qquad x_2 = r\widetilde{\rho}\,\sin\widetilde{\theta}\,\sin\varphi, \qquad x_3 = r\widetilde{\rho}\,\cos\widetilde{\theta}.$$

Then $\mathcal{C}'(r, r_0, \alpha)$ can be expressed as

$$\mathcal{C}'(r, r_0, \alpha) = \left\{(\widetilde{\rho}, \widetilde{\theta}, \varphi) : 1 \leqslant \widetilde{\rho} \leqslant \frac{r_0}{r}, 0 \leqslant \theta \leqslant \widetilde{\alpha}(\varphi, \widetilde{\rho}), 0 \leqslant \varphi \leqslant 2\pi\right\},$$

for some $\widetilde{\alpha}$ satisfying $\widetilde{\alpha}(\varphi, \widetilde{\rho}) < \alpha_2$ and $\widetilde{\alpha}(\varphi, 1) = 0$.

By taking the integral of $\frac{x_3(-9x_1^2 - 9x_2^2 + 6x_3^2)}{|x|^7}$ in $\mathcal{C}'(r, r_0, \alpha)$ for small r, we get

$$\int_{\mathcal{C}'(r,r_0,\alpha)} \frac{x_3(-9x_1^2-9x_2^2+6x_3^2)}{|x|^7}\mathrm{d}x$$
$$= r^{-1}\int_1^{r_0/r}\mathrm{d}\widetilde{\rho}\int_0^{2\pi}\mathrm{d}\varphi\int_0^{\widetilde{\alpha}(\varphi,\widetilde{\rho})}\mathrm{d}\widetilde{\theta}\left[\widetilde{\rho}^{-2}\ \sin\widetilde{\theta}\ \cos\widetilde{\theta}(-9\sin^2\widetilde{\theta}+6\cos^2\widetilde{\theta})\right]. \tag{7}$$

Next we will bound the above integral from below for $r>0$ small. For any $\widetilde{\rho}\in[1,\frac{r_0}{r}]$ and $\varphi\in[0,2\pi]$, since $\widetilde{\alpha}(\varphi,\widetilde{\rho})\in[0,\frac{\pi}{2}]$, we have

$$\begin{aligned}&\int_0^{\widetilde{\alpha}(\varphi,\widetilde{\rho})}\left[\sin\widetilde{\theta}\ \cos\widetilde{\theta}\left(-9\sin^2\widetilde{\theta}+6\cos^2\widetilde{\theta}\right)\right]\mathrm{d}\widetilde{\theta}\\&\quad=3\left(\cos^3\widetilde{\theta}-\cos^5\widetilde{\theta}\right)\Big|_0^{\widetilde{\alpha}(\varphi,\widetilde{\rho})}\\&\quad=3\cos^3\widetilde{\alpha}(\varphi,\widetilde{\rho})-3\cos^5\widetilde{\alpha}(\varphi,\widetilde{\rho})\\&\quad\geqslant 0.\end{aligned}$$

By elementary geometry, we have for any $\widetilde{\rho}>2$ that

$$0<\frac{\alpha_1}{2}<\frac{\alpha(\varphi)}{2}<\widetilde{\alpha}(\varphi,\widetilde{\rho})<\alpha(\varphi)<\alpha_2<\frac{\pi}{2},$$

which is illustrated in figure 3(B), and then

$$\begin{aligned}&\int_0^{\widetilde{\alpha}(\varphi,\widetilde{\rho})}\left[\sin\widetilde{\theta}\ \cos\widetilde{\theta}\left(-9\sin^2\widetilde{\theta}+6\cos^2\widetilde{\theta}\right)\right]\mathrm{d}\widetilde{\theta}\\&\quad=3\cos^3\widetilde{\alpha}(\varphi,\widetilde{\rho})-3\cos^5\widetilde{\alpha}(\varphi,\widetilde{\rho})\\&\quad\geqslant 3\ \min\left\{\cos^3\frac{\alpha_1}{2}-\cos^5\frac{\alpha_1}{2},\cos^3\alpha_2-\cos^5\alpha_2\right\}\\&\quad>0,\end{aligned}$$

for $\widetilde{\rho}>2$. Thus we obtain

$$\begin{aligned}&\int_1^{+\infty}\mathrm{d}\widetilde{\rho}\int_0^{2\pi}\mathrm{d}\varphi\int_0^{\widetilde{\alpha}(\varphi,\widetilde{\rho})}\mathrm{d}\widetilde{\theta}\left[\widetilde{\rho}^{-2}\ \sin\widetilde{\theta}\ \cos\widetilde{\theta}\left(-9\sin^2\widetilde{\theta}+6\cos^2\widetilde{\theta}\right)\right]\\&\quad\geqslant\int_2^{+\infty}\mathrm{d}\widetilde{\rho}\int_0^{2\pi}\mathrm{d}\varphi\int_0^{\widetilde{\alpha}(\varphi,\widetilde{\rho})}\mathrm{d}\widetilde{\theta}\left[\widetilde{\rho}^{-2}\ \sin\widetilde{\theta}\ \cos\widetilde{\theta}\left(-9\sin^2\widetilde{\theta}+6\cos^2\widetilde{\theta}\right)\right]\\&\quad\geqslant C_0,\end{aligned}$$

where the constant $C_0>0$ depends on α_1,α_2. We also have

$$\begin{aligned}&\left|\int_{r_0/r}^{+\infty}\mathrm{d}\widetilde{\rho}\int_0^{2\pi}\mathrm{d}\varphi\int_0^{\widetilde{\alpha}(\varphi,\widetilde{\rho})}\mathrm{d}\widetilde{\theta}\left[\widetilde{\rho}^{-2}\ \sin\widetilde{\theta}\ \cos\widetilde{\theta}(-9\sin^2\widetilde{\theta}+6\cos^2\widetilde{\theta})\right]\right|\\&\quad\leqslant C'\left|\int_{r_0/r}^{\infty}\widetilde{\rho}^{-2}\,\mathrm{d}\widetilde{\rho}\right|\leqslant C'r,\end{aligned}$$

where C' is a positive constant. Therefore

$$\begin{aligned}
&\int_1^{r_0/r} \mathrm{d}\widetilde{\rho}\int_0^{2\pi} \mathrm{d}\varphi\int_0^{\widetilde{\alpha}(\varphi,\widetilde{\rho})} \mathrm{d}\widetilde{\theta}\left[\widetilde{\rho}^{-2}\,\sin\,\widetilde{\theta}\,\cos\,\widetilde{\theta}\left(-9\sin^2\widetilde{\theta}+6\cos^2\widetilde{\theta}\right)\right]\\
&\quad\geqslant \int_1^{+\infty} \mathrm{d}\widetilde{\rho}\int_0^{2\pi} \mathrm{d}\varphi\int_0^{\widetilde{\alpha}(\varphi,\widetilde{\rho})} \mathrm{d}\widetilde{\theta}\left[\widetilde{\rho}^{-2}\,\sin\,\widetilde{\theta}\,\cos\,\widetilde{\theta}\left(-9\sin^2\widetilde{\theta}+6\cos^2\widetilde{\theta}\right)\right]\\
&\qquad-\left|\int_{r_0/r}^{+\infty} \mathrm{d}\widetilde{\rho}\int_0^{2\pi} \mathrm{d}\varphi\int_0^{\widetilde{\alpha}(\varphi,\widetilde{\rho})} \mathrm{d}\widetilde{\theta}\left[\widetilde{\rho}^{-2}\,\sin\,\widetilde{\theta}\,\cos\,\widetilde{\theta}\left(-9\sin^2\widetilde{\theta}+6\cos^2\widetilde{\theta}\right)\right]\right|\\
&\quad\geqslant C_0 - C'\,r.
\end{aligned}$$

Using the above estimate and (7), we have

$$\int_{\mathcal{C}'(r,r_0,\alpha)} \Phi(x)\mathrm{d}x \geqslant C_0 r^{-1} - C_1|\log\,r|, \tag{8}$$

where $C_0 > 0, C_1$ depend on $\alpha_1, \alpha_2, r_0, \kappa$, and we have used the asymptotics of Φ given in (6) and the fact that

$$\int_{\mathcal{C}'(r,r_0,\alpha)} |x|^{-3}\,\mathrm{d}x \leqslant C\int_{B_{r_0}\setminus B_r} |x|^{-3}\,\mathrm{d}x \leqslant C\int_r^{r_0} \rho^{-3}\rho^2\,\mathrm{d}\rho \leqslant C|\log\,r|.$$

For $x \neq y$, we define

$$G(x,y) := G(x-y)$$

and

$$\Phi(x,y) := \Phi(x-y) = -\,\mathrm{Im}(\partial^3_{x_3}G(x,y)) = -\,\mathrm{Im}(\partial^3_{x_3}G(x-y)). \tag{9}$$

It is easy to verify that

$$\Phi(y,x) = \Phi(y-x) = -\,\mathrm{Im}(\partial^3_{y_3}G(x-y)) = -\Phi(x,y) = -\Phi(x-y).$$

For fixed y, it is clear to see that the function $\Phi(\cdot,y)$ is singular at $x=y$ and satisfies the Helmholtz equation for $x \neq y$.

Remark 2. The estimate (8) with the constant $C_0 > 0$ is crucial for the proof of the main theorem. We can not have a positive C_0 near a facet point, for which $\alpha \equiv \alpha_2 = \frac{\pi}{2}$.This is the fact that corners always have strong scattering effects [17, 19]. Therefore, we will be essentially using 'corner scattering' to do the recovery. We refer to [18, 23] for similar approaches to recover piecewise constant coefficients. We believe that one can also use 'edge scattering' to serve our purposes.

3. Proof of the main result

In this section, we show the proof of the main result which is stated in theorem 1. First we define a sequence of domains which will be used in the proof.

Let

$$U_0 = \Omega, \qquad W_0 = \emptyset, \qquad U_k = \Omega\setminus\cup_{j=1}^k D_j, \qquad W_k = \Omega\setminus U_k, \quad k = 1,\ldots,N.$$

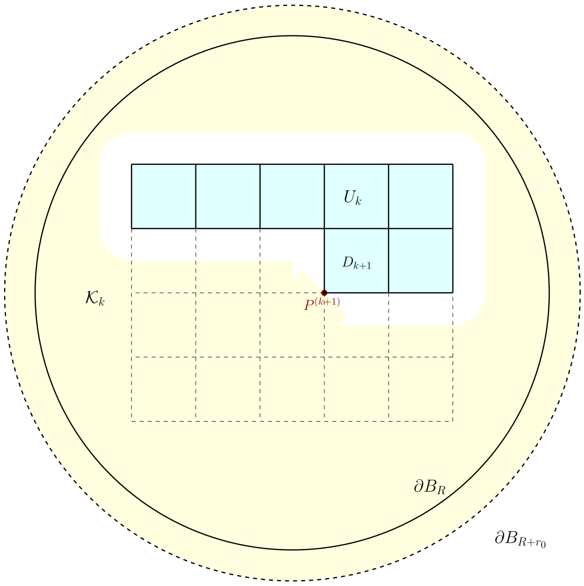

Figure 4. The domains U_k and $\mathcal{K}_k$ for $k = 13$.

For each $k \in \{0, 1, 2, \ldots, N-1\}$, consider the vertex $P^{(k+1)}$ of the cell D_{k+1}. By choosing appropriate Cartesian coordinates $(x_1^{(k+1)}, x_3^{(k+1)}, x_3^{(k+1)})$, we assume $D_{k+1} \cap B_{r_0}(P^{(k+1)}) = P^{(k+1)} + \mathcal{C}(r_0, \alpha^{(k+1)})$, with $\alpha^{(k+1)} = \alpha^{(k+1)}(\varphi)$, $\varphi \in [0, 2\pi]$, i.e., a cone with vertex at $P^{(k+1)}$. By assumption 2, we have

$$\alpha_1 < \alpha^{(k+1)}(\varphi) < \alpha_2$$

for $\varphi \in [0, 2\pi]$.

Denote $P^{(k+1)} = (p_1^{(k+1)}, p_2^{(k+1)}, p_3^{(k+1)})$,

$$Q_{k+1}^{-} = \Big\{ x = (x_1^{(k+1)}, x_2^{(k+1)}, x_3^{(k+1)}) : |x_1^{(k+1)} - p_1^{(k+1)}|^2 \\ + |x_2^{(k+1)} - p_2^{(k+1)}|^2 < r_0^2, , -2r_0 < x_3^{(k+1)} - p_3^{(k+1)} < 0 \Big\},$$

and

$$\mathcal{K}_k = \{x \in B_{R+r_0} : \mathrm{dist}(x, U_k) > r_0\} \cup Q_{k+1}^{-}.$$

We note that $\mathcal{K}_k$ is connected under assumption 1. Figure 4 shows an illustrative example of the domains U_k and $\mathcal{K}_k$.

3.1. Unique continuation

We state a quantitative estimate of unique continuation for the solution of the Helmholtz equation. The proof is omitted since it is a minor modification of the proof for a similar estimate in [13, proposition 3.9] and [16, proposition 7]. We remark that the proof is based on the construction of a pathway and the repeated use of three spheres inequalities under assumption 1.

Proposition 1. *Let $\mathcal{K}_k$ be defined as before and let $v \in H^1(\mathcal{K}_k)$ be a weak solution to the Helmholtz equation*

$$\Delta v + \kappa^2 v = f \quad \text{in } \mathcal{K}_k.$$

Assume that, for given positive constants ε_0 and E_1, v satisfies

$$\|v\|_{L^\infty\left(B_{R+r_0}\setminus B_{R+\frac{r_0}{2}}\right)} \leqslant \varepsilon_0$$

and

$$|v(x)| \leqslant E_1 |x - P^{(k+1)}|^{-1}, \quad x \in \mathcal{K}_k.$$

Then the following inequality holds for small enough $r > 0$:

$$|v(x_r)| \lesssim \varepsilon^{\tau_r} E_1^{1-\tau_r} r^{-(1-\tau_r)},$$

where $x_r = P^{(k+1)} + (0, 0, -r)$ and $\tau_r = \theta r^\delta$ with $0 < \theta < 1$ and $\delta > 0$ depending on r_0, κ, N, A.

3.2. Proof of theorem 1

For some $k \in \{0, 1, \ldots, N-1\}$, let

$$\Phi_k(x, y) := -\operatorname{Im}(\partial^3_{x_3^{(k+1)}} G(x - y)).$$

For a fixed k, we just denote the Cartesian coordinates $(x_1, x_2, x_3) = (x_1^{(k+1)}, x_3^{(k+1)}, x_3^{(k+1)})$ for brevity. In the following, we work exclusively under this coordinate system. Note that, under these coordinates, formally we have

$$\Phi_k(x, y) = \Phi(x - y).$$

where $\Phi(\cdot, \cdot)$ is defined in (9).

Define

$$S_k(y) = \int_{U_k} f(x)\Phi_k(x, y)\mathrm{d}x.$$

Lemma 1. *For $y \in \mathcal{K}_k$, it holds that $(\Delta + \kappa^2)S_k(y) = 0$.*

Proof. Noting that for any $x \in U_k$, $y \in \mathcal{K}_k$, we have

$$\begin{aligned} f(x)(\Delta_y + \kappa^2)\Phi_k(x, y) &= -f(x)(\Delta_y + \kappa^2)\operatorname{Im}(\partial^3_{x_3} G(x - y)) \\ &= -f(x)\partial^3_{x_3} \operatorname{Im}((\Delta_y + \kappa^2)G(x - y)) \\ &= 0, \end{aligned}$$

since U_k and $\mathcal{K}_k$ are disconnected. The proof is completed if we change the order of integration and differentiation. $\square$

Lemma 2. *If for some* $\varepsilon_0 > 0$ *and* $k \in \{1, \ldots, N-1\}$, *it holds*

$$|S_k(y)| \leqslant \varepsilon_0, \quad \forall\, y \in B_{R+r_0} \setminus B_{R+\frac{r_0}{2}},$$

then

$$|S_k(y_r)| \lesssim E^{1-\tau_r}\varepsilon_0^{\tau_r} r^{-(1-\tau_r)},$$

where $y_r = P^{(k+1)} + (0, 0, -r)$ *with* r *being small enough and* $\tau_r = \theta r^{\delta}$ *with the positive constants* $\theta \in (0, 1)$ *and* δ *depending on* r_0, κ, N, A.

Proof. It follows from lemma 1 that S_k satisfies $(\Delta + \kappa^2)S_k(y) = 0$ in $\mathcal{K}_k$. Moreover, by the explicit forms of $S_k(y)$ and $\Phi_k(x, y)$, we have

$$|S_k(y)| \leqslant CE\int_{U_k} \frac{1}{|x-y|^4}\mathrm{d}x \leqslant CE\int_{|y-P^{(k+1)}|}^{\infty} \rho^{-2}\,\mathrm{d}\rho \leqslant CE|y - P^{(k+1)}|^{-1},$$

where $C > 0$ is a constant depending on κ, r_0. By proposition 1, we have for $r > 0$ small enough that

$$|S_k(y_r)| \lesssim E^{1-\tau_r}\varepsilon_0^{\tau_r} r^{-(1-\tau_r)},$$

which completes the proof. □

Multiplying both sides of (1) by $\Phi_k(x, y)$ for $y \in B_{R+r_0} \setminus B_{R+\frac{r_0}{2}}$ and using integration by parts, we have

$$\begin{aligned}
\int_{\Omega} f(x)\Phi_k(x, y)\mathrm{d}x &= \int_{B_R} f(x)\Phi_k(x, y)\mathrm{d}x \\
&= \int_{B_R} \left[(\Delta + \kappa^2)u(x)\right]\Phi_k(x, y)\mathrm{d}x \\
&= \int_{B_R} u(x)(\Delta_x + \kappa^2)\Phi_k(x, y)\mathrm{d}x \\
&\quad + \int_{\partial B_R} \left[\partial_{\nu(x)}u(x)\Phi_k(x, y) - \partial_{\nu(x)}\Phi_k(x, y)u(x)\right]\mathrm{d}s \\
&= \int_{\partial B_R} \left[\partial_{\nu(x)}u(x)\Phi_k(x, y) - \partial_{\nu(x)}\Phi_k(x, y)u(x)\right]\mathrm{d}s, \qquad (10)
\end{aligned}$$

where ν is the unit outer normal vector on ∂B_R.

First, note that for $k = 0$,

$$S_0(y) = \int_{\Omega} f(x)\Phi_0(x, y)\mathrm{d}x.$$

Also notice that

$$\int_{\partial B_R} |\Phi_0(\cdot, y)|^2 + |\partial_\nu \Phi_0(\cdot, y)|^2\,\mathrm{d}s \leqslant C$$

for $y \in B_{R+r_0} \setminus B_{R+\frac{r_0}{2}}$, where C depends on R, κ, r_0. Notice that $u|_{\mathbb{R}^3\setminus B_R}$ is the solution to the exterior problem for the Helmholtz equation

$$\Delta u + \kappa^2 u = 0 \quad \text{in } \mathbb{R}^3 \setminus B_R$$

along with the radiation condition (2). For the above exterior problem, it is shown in [36, theorem 2.6.4] that there exists a bounded operator $\mathcal{N} : H^1(\partial B_R) \to L^2(\partial B_R)$, which is called exterior Dirichlet-to-Neumann map, such that

$$\partial_\nu u = \mathcal{N} u \quad \text{on } \partial B_R.$$

Hence, the Neumann data $\partial_\nu u$ on ∂B_R can be obtained once the Dirichlet date u is available on ∂B_R. Therefore, we obtain the following estimate

$$\begin{aligned}\int_{\partial B_R} \left(|\partial_\nu u|^2 + \kappa^2 |u|^2\right) \mathrm{d}s &= \int_{\partial B_R} \left(|\mathcal{N} u|^2 + \kappa^2 |u|^2\right) \mathrm{d}s \\ &\leqslant C\|u\|^2_{H^1(\partial B_R)} \leqslant C\epsilon^2,\end{aligned}$$

where C depends on κ and R. Therefore by (10), we obtain

$$|S_0(y)| \lesssim \epsilon, \quad y \in B_{R+r_0} \setminus B_{R+\frac{r_0}{2}}. \tag{11}$$

First we prove a logarithmic-type stability. Denote $\delta_0 = \epsilon$ and $\delta_j = \|f\|_{L^\infty(W_j)}, j = 1, \ldots, N$. We will inductively prove that the following estimates hold:

$$\delta_j \leqslant \omega_j(\epsilon), \tag{12}$$

where $\omega_0(\epsilon) \leqslant \omega_1(\epsilon) \leqslant \cdots \leqslant \omega_N(\epsilon)$ for any small $\epsilon > 0$ and

$$\lim_{\epsilon \to 0} \omega_j(\epsilon) = 0$$

for each j. The estimate (12) is clearly true for $j = 0$, for which $\omega_0(\epsilon) = \epsilon$, by invoking (11). We now assume that the estimate (12) is true for $j = k$, and deduce the estimate for $j = k + 1$.

Recall that

$$\begin{aligned}S_k(y) &= \int_{U_k} f(x)\Phi_k(x, y)\mathrm{d}x \\ &= \int_\Omega f(x)\Phi_k(x, y)\mathrm{d}x - \int_{W_k} f(x)\Phi_k(x, y)\mathrm{d}x.\end{aligned}$$

Thus we have the estimate

$$|S_k(y)| \leqslant \left| \int_\Omega f(x)\Phi_k(x, y)\mathrm{d}x \right| + \left| \int_{W_k} f(x)\Phi_k(x, y)\mathrm{d}x \right|. \tag{13}$$

Similar to (11), we have

$$\left| \int_\Omega f(x)\Phi_k(x, y)\mathrm{d}x \right| \leqslant C\epsilon \tag{14}$$

for $y \in B_{R+r_0} \setminus B_{R+\frac{r_0}{2}}$. For the estimate of the second term in the right-hand side of (13), first notice that $|x - y| > Cr_0$ for $x \in W_k$ and $y \in B_{R+r_0} \setminus B_{R+\frac{r_0}{2}}$, and therefore

$$|\Phi_k(x, y)| \leqslant \frac{C}{|x - y|^4} \leqslant \frac{C}{r_0^4}.$$

Also we have $|f(x)| \leqslant C\omega_k(\epsilon)$ for $x \in W_k$ by the hypothesis for induction. Therefore

$$\left|\int_{W_k} f(x)\Phi_k(x,y)\mathrm{d}x\right| \leqslant C\omega_k(\epsilon) \tag{15}$$

for $y \in B_{R+r_0} \setminus B_{R+\frac{r_0}{2}}$. Combining the estimates (13)–(15), we obtain

$$|S_k(y)| \lesssim (\epsilon + \omega_k(\epsilon)), \quad y \in B_{R+r_0} \setminus B_{R+\frac{r_0}{2}}.$$

Note that the above estimate is also valid for $k = 0$, for which $W_0 = \emptyset$. Now let $y_r = P^{(k+1)} + (0, 0, -r)$. By lemma 2, we have

$$|S_k(y_r)| \lesssim r^{-1}\omega_k(\epsilon)^{\tau_r}, \tag{16}$$

if $0 < r < \frac{1}{C_2}$ for some constant $C_2 > 0$.

Next, we write

$$S_k(y_r) = I_1 + I_2,$$

where

$$I_1 = \int_{B_{r_0}(y_r)\cap D_{k+1}} f(x)\Phi_k(x,y_r)\mathrm{d}x,$$

$$I_2 = \int_{U_k\setminus(B_{r_0}(y_r)\cap D_{k+1})} f(x)\Phi_k(x,y_r)\mathrm{d}x.$$

The region $B_{r_0}(y_r) \cap D_{k+1}$ is depicted in figure 5. First it is easy to verify that

$$|I_2| \lesssim 1. \tag{17}$$

Combining (16) and (17) yields

$$|I_1| \lesssim r^{-1}\omega_k(\epsilon)^{\tau_r} + 1. \tag{18}$$

Since $f(x) = c_{k+1}$ on D_{k+1}, we have

$$|I_1| = |c_{k+1}| \left|\int_{B_{r_0}(y_r)\cap D_{k+1}} \Phi_k(x,y_r)\mathrm{d}x\right|.$$

By (8), we have

$$\left|\int_{B_{r_0}(y_r)\cap D_{k+1}} \Phi_k(x,y_r)\mathrm{d}x\right| = \left|\int_{\mathcal{C}'(r,r_0,\alpha^{(k+1)})} \Phi(x)\mathrm{d}x\right| \geqslant C_0 r^{-1} - C_1 r^{-1/2},$$

where C_0, C_1 two positive constants. Together with (18), we obtain

$$C_0|c_{k+1}|r^{-1} \lesssim |I_1| + r^{-1/2} \leqslant r^{-1}\omega_k(\epsilon)^{\tau_r} + r^{-1/2}.$$

Multiplying above inequality by r gives

$$|c_{k+1}| \lesssim \omega_k(\epsilon)^{\tau_r} + r^{1/2},$$

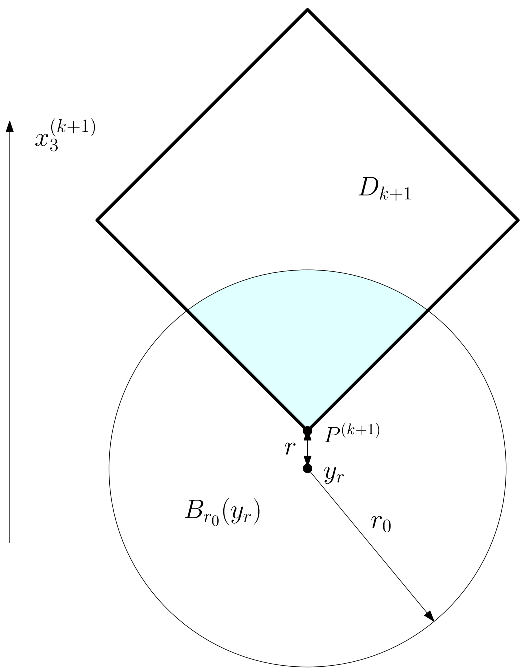

Figure 5. The shaded region is $B_{r_0}(y_r) \cap D_{k+1}$.

where $r \in (0, \frac{1}{C_2})$. Define

$$\sigma(t) = \begin{cases} |\log t|^{-\frac{1}{4\delta}} & \text{for } 0 < t < \mathrm{e}^{-1}, \\ t - \mathrm{e}^{-1} + 1 & \text{for } t > \mathrm{e}^{-1}. \end{cases}$$

If $\omega_k(\epsilon) < \mathrm{e}^{-1}$, by taking

$$r = \frac{|\log \omega_k(\epsilon)|^{-\frac{1}{2\delta}}}{C_2} < \frac{1}{C_2},$$

we obtain

$$|c_{k+1}| \lesssim |\log \omega_k(\epsilon)|^{-\frac{1}{4\delta}} = \sigma(\omega_k(\epsilon)).$$

Remember that $\delta > 0$ depends on r_0, κ, N, A. If $\omega_k(\epsilon) > \mathrm{e}^{-1}$, we have

$$|c_{k+1}| \lesssim \sigma(\omega_k(\epsilon))$$

since $|c_{k+1}|$ is bounded. Hence

$$\delta_{k+1} \lesssim \omega_{k+1}(\epsilon) := \sigma(\omega_k(\epsilon)).$$

Then it is easy to verify that $\lim_{\epsilon\to 0} \omega_{k+1}(\epsilon) = 0$, which completes the induction. Now we conclude that there exists some positive constant C^* such that

$$\|f\|_{L^\infty(\Omega)} \leqslant C^* \omega_N(\epsilon), \tag{19}$$

where $\lim_{\epsilon\to 0}\omega_N(\epsilon)=0$. Notice that $\omega_N(\cdot):(0,\infty)\to(0,\infty)$ is monotonically increasing.

The final Lipschitz-type stability is an almost immediate consequence of (19) since we are recovering a finite number of parameters. We refer to [11, proposition 5] and [21, theorem 2.1 and remark 2.2] for more details.

More precisely, we consider the linear operator $T:\mathbb{C}^N\to H^1(\partial B_R)$ such that

$$T(c_1,\dots,c_N)\mapsto u|_{\partial B_R},$$

where u solves (1) with f being given by the form (4). The boundedness of T follows directly from (3). By (19), we have

$$\inf_{\|(c_1,\dots,c_N)\|_\infty=E}\|T(c_1,\dots,c_N)\|_{H^1(\partial B_R)}\geqslant\omega_N^{-1}\left(\frac{E}{C^*}\right)=:C''>0,$$

and then

$$\|T(c_1,\dots,c_N)\|_{H^1(\partial B_R)}\gtrsim\max_{1\leqslant j\leqslant N}\|c_j\|.$$

This completes the proof of theorem 1.

4. Conclusion

We have presented the Lipschitz stability for the inverse source scattering problem of the three-dimensional Helmholtz equation in a homogeneous background medium, where the source is assumed be a piecewise constant function. The analysis requires the Dirichlet data only. The proof relies on the construction of singular solutions and the quantitative estimate of unique continuation of the solutions for elliptic-type equations. A possible continuation of this work is to study the corresponding stability estimates of the inverse source problems for elastic and electromagnetic waves, where the fundamental solutions are tensors and therefore more sophisticated analysis is needed. We will report the progress elsewhere in the future.

Acknowledgments

The authors want to express their sincere gratitude to the referees whose invaluable comments have helped to improve this paper.

ORCID iDs

Peijun Li https://orcid.org/0000-0001-5119-6435
Jian Zhai https://orcid.org/0000-0002-2374-8922
Yue Zhao https://orcid.org/0000-0001-5939-8410

References

[1] Acosta S, Chow S, Taylor J and Villamizar V 2012 On the multi-frequency inverse source problem in heterogeneous media *Inverse Problems* **28** 075013

[2] Alberti G and Santacesaria M 2019 Calderón's inverse problem with a finite number of measurements *Forum Math., Sigma* **7** 1–20

[3] Alessandrini G, de Hoop M V, Gaburro R and Sincich E 2017 Lipschitz stability for the electrostatic inverse boundary value problem with piecewise linear conductivities *J. Math. Pures Appl.* **107** 638–64
[4] Alessandrini G and Vessella S 2005 Lipschitz stability for the inverse conductivity problem *Adv. Appl. Math.* **35** 207–41
[5] Bao G, Ammari H and Fleming J L 2002 An inverse source problem for Maxwell's equations in magnetoencephalography *SIAM J. Appl. Math.* **62** 1369–82
[6] Badia A E and Nara T 2011 An inverse source problem for Helmholtz's equation from the Cauchy data with a single wave number *Inverse Problems* **27** 105001
[7] Bao G, Li P, Lin J and Triki F 2015 Inverse scattering problems with multi-frequencies *Inverse Problems* **31** 093001
[8] Bao G, Lin J and Triki F 2010 A multi-frequency inverse source problem *J. Differ. Equ.* **249** 3443–65
[9] Bao G, Li P and Zhao Y 2020 Stability for the inverse source problems in elastic and electromagnetic waves *J. Math. Pures Appl.* **134** 122–78
[10] Bao G, Lu S, Rundell W and Xu B 2015 A recursive algorithm for multifrequency acoustic inverse source problems *SIAM J. Numer. Anal.* **53** 1608–28
[11] Bacchelli V and Vessella S 2006 Lipschitz stability for a stationary 2D inverse problem with unknown polygonal boundary *Inverse Problems* **22** 1627–58
[12] Beretta E, de Hoop M V, Francini E, Vessella S and Zhai J 2017 Uniqueness and Lipschitz stability of an inverse boundary value problem for time-harmonic elastic waves *Inverse Problems* **33** 035013
[13] Beretta E, de Hoop M V and Qiu L 2013 Lipschitz stability of an inverse boundary value problem for a Schrödinger-type equation *SIAM J. Math. Anal.* **45** 679–99
[14] Beretta E and Francini E 2011 Lipschitz stability for the electrical impedance tomography problem: the complex case *Commun. PDE* **36** 1723–49
[15] Beretta E, Francini E, Morassi A, Rosset E and Vessella S 2014 Lipschitz continuous dependence of piecewise constant Lamé coefficients from boundary data: the case of non-flat interfaces *Inverse Problems* **30** 125005
[16] Beretta E, Francini E and Vessella S 2014 Uniqueness and Lipschitz stability for the identification of Lamé parameters from boundary measurements *Inverse Problems Imaging* **8** 611–44
[17] Blåsten E 2018 Nonradiating sources and transmission eigenfunctions vanish at corners and edges *SIAM J. Math. Anal.* **50** 6255–70
[18] Blåsten E and Liu H 2020 Recovering piecewise constant refractive indices by a single far-field pattern *Inverse Problems* **36** 085005
[19] Blåsten E, Päivärinta L and Sylvester J 2014 Corners always scatter *Commun. Math. Phys.* **331** 725–53
[20] Bleistein N and Cohen J K 1977 Nonuniqueness in the inverse source problem in acoustics and electromagnetics *J. Math. Phys.* **18** 194–201
[21] Bourgeois L 2013 A remark on Lipschitz stability for inverse problems *C. R. Math.* **351** 187–90
[22] Calderón A-P 1980 On an inverse boundary value problem *Seminar on Numerical Analysis and its Applications to Continuum Physics* (Rio de Janeiro 1980) (Rio de Janeiro: Sociedade Brasileira de Matemática)
[23] Cao X, Diao H and Liu H 2020 Determining a piecewise conductive medium body by a single far-field measurement (arXiv:2005.04420)
[24] Cheng J, Isakov V and Lu S 2016 Increasing stability in the inverse source problem with many frequencies *J. Differ. Equ.* **260** 4786–804
[25] Colton D and Kress R 1998 *Inverse Acoustic and Electromagnetic Scattering Theory* (Berlin: Springer)
[26] Elschner J and Hu G 2018 Acoustic scattering from corners, edges and circular cones *Arch. Ration. Mech. Anal.* **228** 653–90
[27] Friedman A and Isakov V 1989 On the uniqueness in the inverse conductivity problem with one measurement *Indiana Univ. Math. J.* **38** 563–79
[28] Fokas A S, Kurylev Y and Marinakis V 2004 The unique determination of neuronal currents in the brain via magnetoencephalography *Inverse Problems* **20** 1067–82
[29] Harrach B 2019 Uniqueness and Lipschitz stability in electrical impedance tomography with finitely many electrodes *Inverse Problems* **35** 024005
[30] Hu G and Li J 2019 Uniqueness to inverse source problems in an inhomogeneous medium with a single far-field pattern (arXiv:1907.08390v2)

[31] Ikehata M 1999 Reconstruction of a source domain from the Cauchy data *Inverse Problems* **15** 637–45
[32] Kusiak S and Sylvester J 2003 The scattering support *Commun. Pure Appl. Math.* **56** 1525–48
[33] Li P and Yuan G 2017 Increasing stability for the inverse source scattering problem with multi-frequencies *Inverse Problems Imaging* **11** 745–59
[34] Li P, Zhai J and Zhao Y 2020 Stability for the acoustic inverse source problem in inhomogeneous media *SIAM J. Appl. Math.* **80** 2547–59
[35] Liu H and Tsou C-H 2020 Stable determination of polygonal inclusions in Calderon's problem by a single partial boundary measurement *Inverse Problems* **36** 1–24
[36] Nédélec J-C 2000 *Acoustic and Electromagnetic Equations: Integral Representations for Harmonic Problems* (New York: Springer)
[37] Rondi L 2006 A remark on a paper by Alessandrini and Vessella *Adv. Appl. Math.* **36** 67–9
[38] Rüland A, Sincich E and Sincich E 2019 Lipschitz stability for the finite dimensional fractional Calderón problem with finite Cauchy data *Inverse Problems Imaging* **13** 1023–44
[39] Sylvester J 2006 Notions of support for far fields *Inverse Problems* **22** 1273–88
[40] Sylvester J and Uhlmann G 1987 A global uniqueness theorem for an inverse boundary value problem *Ann. Math.* **125** 153–69